Tunable magnomechanically induced transparency and fast-slow light in a hybrid cavity magnomechanical system

Qinghong Liao(廖庆洪)[1,2,†], Kun Peng(彭坤)[1], and Haiyan Qiu(邱海燕)[1]

[1] *Department of Electronic Information Engineering, Nanchang University, Nanchang* 330031, *China*

[2] *State Key Laboratory of Low-Dimensional Quantum Physics, Department of Physics, Tsinghua University, Beijing* 100084, *China*

(Received 8 August 2022; revised manuscript received 9 December 2022; accepted manuscript online 30 December 2022)

We theoretically explore the tunability of magnomechanically induced transparency (MMIT) phenomenon and fast-slow light effect in a hybrid cavity magnomechanical system in which a high-quality yttrium iron garnet (YIG) sphere and an atomic ensemble are placed inside a microwave cavity. In the probe output spectrum, we can observe magnon-induced transparency (MIT) and MMIT due to the photon-magnon and phonon-magnon couplings. We further investigate the effect of atomic ensemble on the absorption spectrum. The results show that better transparency can be obtained by choosing appropriate atomic ensemble parameters. We give an explicit explanation for the mechanism of the Fano resonance phenomenon. Moreover, we discuss phenomena of slow-light propagation. The maximum group delay increases significantly with the increasing atom–cavity coupling strength, and the conversion between slow light and fast light can also be achieved by adjusting the atom–cavity coupling strength. These results may have potential applications for quantum information processing and high precision measurements.

Keywords: magnomechanical system, atomic ensemble, magnomechanically induced transparency, fast and slow light

PACS: 42.50.–p, 42.50.Nn, 42.50.Ct, 42.50.Md **DOI:** 10.1088/1674-1056/acaf2b

1. Introduction

Light-matter interaction has become an active and important research topic, which generally has potential applications in many fields, e.g., optomechanically induced transparency (OMIT),[1–4] coherent manipulation of light,[5,6] electromagnetically induced transparency (EIT),[7–12] and the entanglement preparation between the cavity field and the macroscopic oscillator.[13–15] In the past decade, it promoted the development of solid quantum memory and quantum information processing. EIT is a typical quantum interference effect, which occurs in three-level atoms.[16] It refers to the fact that the absorption rate of atoms can be reduced to zero under the action of an auxiliary laser field, which is mainly caused by interference effects or dark state resonance in an excited state. Moreover, the EIT analogs due to the destructive interference of the anti-Stokes scattering field and the weak probe field are called OMIT.[17] This phenomenon has been extensively studied both experimentally[1,2] and theoretically.[3,4] Up to date, due to emergence of various novel cavity optomechanical systems, the multiple-OMIT phenomenon has been researched theoretically in hybrid piezo-optomechanical cavity systems,[18] atomic-media assisted optomechanical systems,[13,19] and multiple-resonator optomechanical systems,[20] etc.

Recently, analogous to cavity optomechanics, the cavity magnonic system (CMS) with a yttrium iron garnet (YIG) sphere has received increasing interest, which has many benefits over conventional systems. Magnetic materials generally have very low damping rate, high spin density, and high cooperativity with microwave photons,[21–26] thus providing an excellent platform for the study of strong light–matter interaction. In addition to the above merits, the magnon shows an excellent ability to couple with diverse quantum systems, such as optical photons, optical whispering gallery modes (WGMs),[27] microwaves,[28] phonons,[29,30] and superconducting qubits.[31] Thanks to the special features, the systems containing YIG are used to study a variety of coherent phenomena similar to those in optomechanical systems, such as quantum entanglement,[32–34] MMIT,[35] ground-state cooling of magnomechanical resonators,[36–38] fast-slow light engineering,[39–41] bistability and nonreciprocity,[42–44] and so on.

So far, magnetically induced transparency (MIT) has been successfully demonstrated at room temperature, benefiting from the quantum robustness of spin waves to temperature.[23] Magnomechanically induced transparency/absorption (MMIT/MMIA) and magnomechanical parametric amplication (MMPA) are observed in CMS due to magnetostrictive interaction between magnon and phonon.[29] Tunable multiwindow MMIT and magnetically controlled slow-to-fast light conversion have been proposed in the system consisting of two ferromagnetic YIG spheres coupled to a single microwave cavity mode.[35] In addition, the tripartite entanglement and generation of macroscopic quantum coher-

†Corresponding author. E-mail: nculqh@163.com

© 2023 Chinese Physical Society and IOP Publishing Ltd

ence in a typical three-mode coupled cavity magnomechanical system have been studied.[45] Recently, Li *et al.*[46] have proposed a scheme of single-magnon generator via coexistence mechanism of anharmonicity and interference in a hybrid CMS. Other quantum effects like the simultaneous blockade of a photon, phonon, and magnon in a hybrid microwave optomechanical-magnetic system with a two-level atom and a YIG microsphere have also been discussed.[47] Furthermore, many other interesting phenomena have been studied in CMS, such as parity-time-related phenomena,[48,49] tristability,[50] nonreciprocal amplification,[51] and phonon lasing.[52]

Motivated by the above developments, we consider effects of an atomic ensemble on the output spectrum of the CMS in this paper. This work has the following major advantages: the presence of the atomic ensemble can effectively control the width and height of the transparency window. Then, we present a pump-probe optical method to detect the atom–cavity coupling strength. Moreover, the conversion between slow light and fast light can be achieved by adjusting the atom–cavity coupling strength, which provides a scheme for fabrication of optical devices such as all-photonic switches.

The paper is organized as follows. In Section 2, the physical model of our proposal is introduced. In Subsection 3.1, we discuss the MMIT and give an explicit explanation for the mechanism. Furthermore, we analyze the influence of atomic ensemble on the output spectrum. In Subsection 3.2, the Fano resonance in the output field is investigated. The fast-slow light effects in the hybrid cavity magnomechanical system are discussed in Subsection 3.3. Finally, the summary is given in Section 4.

2. Theoretical model and solutions

The hybrid cavity magnomechanical system considered in this paper is schematically shown in Fig. 1(a). A high-quality YIG sphere and an atomic ensemble with N identical two-level atoms are placed inside a microwave cavity.[53–55] The equivalent physical model of the hybrid cavity magnomechanical system is given in Fig. 1(b). The magnon mode is caused by the collective motion of a large number of spins in a ferromagnetic system, e.g., a YIG sphere. In the system, a uniformly biased magnetic field in z-direction is applied on the YIG sphere. The photon mode of the cavity and the magnon mode of YIG are coupled to each other through the magnetic dipole interaction.[23] The phonon mode arises due to the vibrations of the YIG sphere caused by the magnetostrictive force.[29] Therefore the magnon–phonon coupling was established in the YIG sphere. Here, we ignore the Kerr nonlinear effect term of the magnons caused by the magnetocrystalline anisotropy in the YIG sphere.[42] The total Hamiltonian of the magnomechanical system considered here can be written as[35,56]

$$\begin{aligned} H_{\mathrm{T}}/\hbar =\ & \omega_a a^{\dagger}a+\omega_m m^{\dagger}m+\omega_b b^{\dagger}b+\frac{1}{2}\omega_e S_z \\ & +g_1\left(a^{\dagger}m+am^{\dagger}\right)+g_2 m^{\dagger}m\left(b+b^{\dagger}\right) \\ & +g\left(S_+a+S_-a^{\dagger}\right)+\mathrm{i}\Omega\left(m^{\dagger}\mathrm{e}^{-\mathrm{i}\omega_0 t}-m\mathrm{e}^{\mathrm{i}\omega_0 t}\right) \\ & +\mathrm{i}\varepsilon_{\mathrm{p}}\left(a^{\dagger}\mathrm{e}^{-\mathrm{i}\omega_{\mathrm{p}} t}-a\mathrm{e}^{\mathrm{i}\omega_{\mathrm{p}} t}\right), \end{aligned} \tag{1}$$

where $a^{\dagger}\,(a)$, $m^{\dagger}\,(m)$, and $b^{\dagger}\,(b)$ are the creation (annihilation) operators of cavity mode, magnon mode and phonon mode, respectively; ω_a, ω_m, and ω_b are the resonant frequencies of the cavity, magnon and phonon, respectively. It should be pointed out that, ω_m can be tuned by changing the external bias magnetic field H via $\omega_m=\gamma H$. The transition frequency between the ground state $|g\rangle$ and the excited state $|e\rangle$ of a two-level atom is ω_e. The two-level atom collective spin operator is defined as $S_{z,+,-}=\sum_{i=1}^{N}\sigma_{z,+,-}^{i}$, where N is the total number of two-level atoms and $\sigma_{z,+,-}^{i}$ is the operator of the i-th atom, and they satisfy commutation relations $[S_z,S_{\pm}]=\pm 2S_{\pm}$, and $[S_+,S_-]=2S_z$.[57] In the low-excitation limit, the collective spin operator S_z can be approximated as $S_z\simeq\langle S_z\rangle\simeq -N$. The boson annihilation operator for an atom can be defined as $c=S_-/\sqrt{|S_z|}$, which satisfies the commutation relation $\left[c,c^{\dagger}\right]=1$. Here, g is the averaged atom–photon coupling strength.[58] The coupling strength of the magnon with the cavity field (phonon) is described by $g_1\,(g_2)$. The condition for g_1 is as follows: $g_1>\kappa_m,\kappa_a$, where $\kappa_m\,(\kappa_a)$ is the dissipation rate of the magnon (cavity) modes. In contrast, g_2 is considered to be very small but can be enlarged by directly driving the YIG sphere or the cavity mode with a microwave source. The Rabi frequency $\Omega=\frac{\sqrt{5}}{4}\gamma\sqrt{N}B_0$ represents the strength of the driving field with amplitude $B_0=3.9\times10^{-9}$ T and frequency ω_0. The gyromagnetic ratio is $\gamma=28$ GHz/T and the total number of spins is $N=\rho V$ with the spin density of the YIG sphere $\rho=4.22\times10^{27}$ m^{-3} and volume V;[23] ω_{p} is the frequency of the detection field with the amplitude $\varepsilon_{\mathrm{p}}=\sqrt{P_{\mathrm{p}}/\hbar\omega_{\mathrm{p}}}$, P_{p} is the power of a probe field. Note that we can ignore the term $Km^{\dagger}mm^{\dagger}m$ in Eq. (1) which describes the Kerr nonlinear effect when $K\left|\langle m\rangle\right|^3\ll\Omega$.[41]

In a frame rotating at the frequency of the coupling field, we apply a unitary transformation $U(t)=\exp\left[-\mathrm{i}\omega_0\left(a^{\dagger}a+m^{\dagger}m+\frac{1}{2}S_z\right)t\right]$ to the system.[58] The total Hamiltonian of the system can be written as

$$\begin{aligned} H_{\mathrm{eff}}/\hbar =\ & U(t)H_{\mathrm{T}}U^{\dagger}(t)-\mathrm{i}U\frac{\partial}{\partial t}U^{\dagger}(t) \\ =\ & \Delta_a a^{\dagger}a+\Delta_m m^{\dagger}m+\omega_b b^{\dagger}b+\frac{1}{2}\Delta_c S_z \\ & +g_1\left(a^{\dagger}m+am^{\dagger}\right)+g_2 m^{\dagger}m\left(b+b^{\dagger}\right) \\ & +g\left(S_+a+S_-a^{\dagger}\right) \\ & +\mathrm{i}\Omega\left(m^{\dagger}-m\right)+\mathrm{i}\varepsilon_{\mathrm{p}}\left(a^{\dagger}\mathrm{e}^{-\mathrm{i}\delta t}-a\mathrm{e}^{\mathrm{i}\delta t}\right). \end{aligned} \tag{2}$$

Here, the detuning parameters are $\delta=\omega_{\rm p}-\omega_0$, $\Delta_a=\omega_a-\omega_0$, $\Delta_m=\omega_m-\omega_0$, and $\Delta_c=\omega_e-\omega_0$. Introducing the corresponding damping and noise terms, the quantum dynamics of the system can be described by the following Heisenberg–Langevin equations

$$\begin{aligned}\dot{a} &= -\mathrm{i}\Delta_a a-\mathrm{i}g_1 m-\kappa_a a+\varepsilon_{\rm p}\mathrm{e}^{-\mathrm{i}\delta t}\\ &\quad -\mathrm{i}G_a c+\sqrt{2\kappa_a}a^{\rm in}(t), \qquad (3)\\ \dot{m} &= -\mathrm{i}\Delta_m a-\mathrm{i}g_1 a-\kappa_m m-\mathrm{i}g_2 m\left(b+b^{\dagger}\right)\\ &\quad +\Omega+\sqrt{2\kappa_m}m^{\rm in}(t), \qquad (4)\\ \dot{b} &= -\mathrm{i}\omega_b b-\mathrm{i}g_2 m^{\dagger}m-\kappa_b b+\sqrt{2\kappa_b}b^{\rm in}(t), \qquad (5)\\ \dot{c} &= -\gamma_c c-\mathrm{i}\Delta_c c-\mathrm{i}G_a a+\sqrt{2\gamma_c}c^{\rm in}(t), \qquad (6)\end{aligned}$$

where κ_a $(\kappa_m,\kappa_b,\gamma_c)$ is the decay rate of the cavity (magnon, phonon, atoms); $G_a=g\sqrt{N}$ is the coupling strength between the cavity and the collective atomic mode; $a^{\rm in}$, $m^{\rm in}$, $b^{\rm in}$, and $c^{\rm in}$ are the vacuum input noise operators with zero mean, which are fully characterized by nonzero correlation function $\langle q_{\rm in}(t)q_{\rm in}^{\dagger}(t')\rangle=\delta(t-t')$, $q=a,m,b,c$.[59]

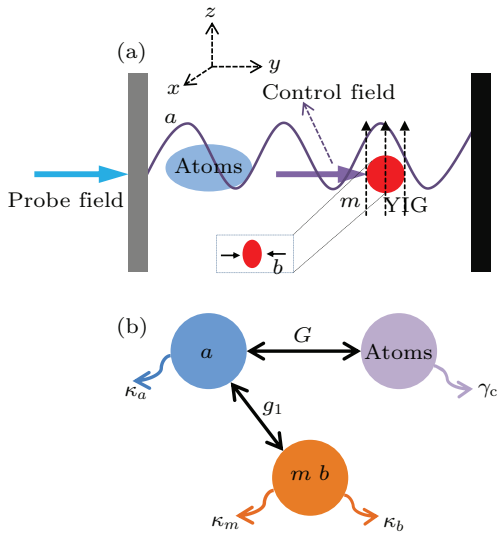


Fig. 1. (a) Schematic of the hybrid cavity magnomechanical system. The cavity traps the atomic ensemble (light blue) and a high-quality YIG sphere (red). (b) The equivalent physical model.

To obtain the amplitude of the probe light, we denote the operator as the sum of quantum fluctuation and steady-state value, i.e., $o=o_{\rm s}+\delta o\,(o=a,m,b,c)$.[60] Therefore, the steady-state solutions of the dynamic operator are obtained as

$$a_{\rm s}=\frac{-\mathrm{i}g_1 m_{\rm s}}{\mathrm{i}\Delta_a+\kappa_a+\frac{G_a^2}{\gamma_c+\mathrm{i}\Delta_c}}, \qquad (7)$$

$$m_{\rm s}=\frac{-\mathrm{i}g_1 a_{\rm s}+\Omega}{\mathrm{i}\tilde{\Delta}_m+\kappa_m}, \qquad (8)$$

$$b_{\rm s}=\frac{-\mathrm{i}g_2|m_{\rm s}|^2}{\mathrm{i}\omega_b+\kappa_b}, \qquad (9)$$

$$c_{\rm s}=\frac{-\mathrm{i}G_a a_{\rm s}}{\gamma_c+\mathrm{i}\Delta_c}, \qquad (10)$$

where $\tilde{\Delta}_m=\Delta_m+g_2\left(b_{\rm s}+b_{\rm s}^*\right)$ is the effective detuning of the driving field and the magnon mode. Further, introducing the linear expansion $o=o_{\rm s}+o_+\mathrm{e}^{-\mathrm{i}\delta t}+o_-\mathrm{e}^{\mathrm{i}\delta t}\,(o=a,m,b,c)$ into Eqs. (3)–(6) and ignoring the resonance term, we obtain the relation satisfied by o_+ as

$$(\mathrm{i}\lambda-\kappa_a)a_+-\mathrm{i}g_1 m_+-\mathrm{i}G_a c_++\varepsilon_{\rm p}=0, \qquad (11)$$

$$(\mathrm{i}\lambda-\kappa_m)m_+-\mathrm{i}g_1 a_+-\mathrm{i}Gb_+=0, \qquad (12)$$

$$(\mathrm{i}\lambda-\kappa_b)b_+-\mathrm{i}G^* m_+=0, \qquad (13)$$

$$(\mathrm{i}\lambda-\gamma_c)c_+-\mathrm{i}G_a a_+=0, \qquad (14)$$

where $G=g_2 m_{\rm s}$ is the effective magnon–phonon coupling strength. In the resolved-sideband regime, we set $\lambda=\delta-\omega_b$ and $\Delta_a=\tilde{\Delta}_m=\Delta_c=\omega_b$. Therefore, we can express the output field response as

$$a_+=\frac{\varepsilon_{\rm p}}{(\mathrm{i}\lambda-\kappa_a)+\frac{g_1^2}{(\mathrm{i}\lambda-\kappa_m)+\frac{|G|^2}{(\mathrm{i}\lambda-\kappa_b)}}+\frac{G_a^2}{(\mathrm{i}\lambda-\gamma_c)}}. \qquad (15)$$

Using the standard input–output relation $\varepsilon_{\rm out}=\varepsilon_{\rm in}-2\kappa_a a$, where $\varepsilon_{\rm in}$ and $\varepsilon_{\rm out}$ are the input field and output field vectors, respectively.[61] The amplitude of the output field oscillating at the probe frequency ω_0 can be written as

$$\varepsilon_{\rm out}=\frac{2\kappa_a a_+}{\varepsilon_{\rm p}}. \qquad (16)$$

The real (imaginary) part of $\varepsilon_{\rm out}$ describes the absorption (dispersion) of the probe field at the probe frequency.

3. Results and discussion

In order to explicitly illustrate the features of the magnomechanically induced transparency and the fast-slow light effect in this hybrid CMS, we analyze the absorption spectrum of the output field using the effective parameters obtained in the cavity magnomechanical system experiments as[29] $\omega_a/2\pi=10$ GHz, $\omega_b/2\pi=10$ MHz, $\omega_m/2\pi=10$ GHz, $\kappa_m/2\pi=0.1$ MHz, $\kappa_a/2\pi=2.1$ MHz, $\kappa_b/2\pi=100$ Hz, $g_1/2\pi=1.5$ MHz, $G/2\pi=1.0$ MHz, $G_a/2\pi=1.0$ MHz.

3.1. Magnomechanically induced transparency

First, under the fixed atom–cavity coupling strength $G_a/2\pi=1.0$ MHz, we consider the effect of the photon-magnon coupling on the probe absorption properties in the hybrid cavity magnomechanical system with the magnon–phonon coupling $G=0$ and $G/2\pi=1.0$ MHz. If the coupling between magnon and phonon is absent, the term $\varepsilon_{\rm out}$ becomes

$$\varepsilon_{\rm out}=\frac{2\kappa_a}{(\mathrm{i}\lambda-\kappa_a)+\frac{g_1^2}{(\mathrm{i}\lambda-\kappa_m)}+\frac{G_a^2}{(\mathrm{i}\lambda-\gamma_c)}}. \qquad (17)$$

In Fig. 2(a), we consider that magnon–phonon coupling is switched off, i.e., $g_2=0$. At this time, there are only the photon-magnon and phonon-atomic couplings. Due to the

magnetic dipole interaction, we can observe that a magnon-induced transparency window appears at resonance $\delta = \omega_b$. As the coupling strength g_1 increases, the transparency window becomes wider and deeper. This indicates that the magnon-induced transparency effect increases with the increase of g_1. Then, we introduce magnon–phonon coupling in Fig. 2(b). Due to the magnetostrictive force interaction, the single MIT window splits into double windows. The reason is that the MMIT window is obtained when the phonon-magnon coupling is introduced. Similar to Fig. 2(a), the transparency windows become wider and deeper with the increase of g_1. This shows that MIT and MMIT are enhanced with the increase of photon-magnon coupling. Therefore, the width of the transparent window can be controlled by changing the photon-magnon coupling.

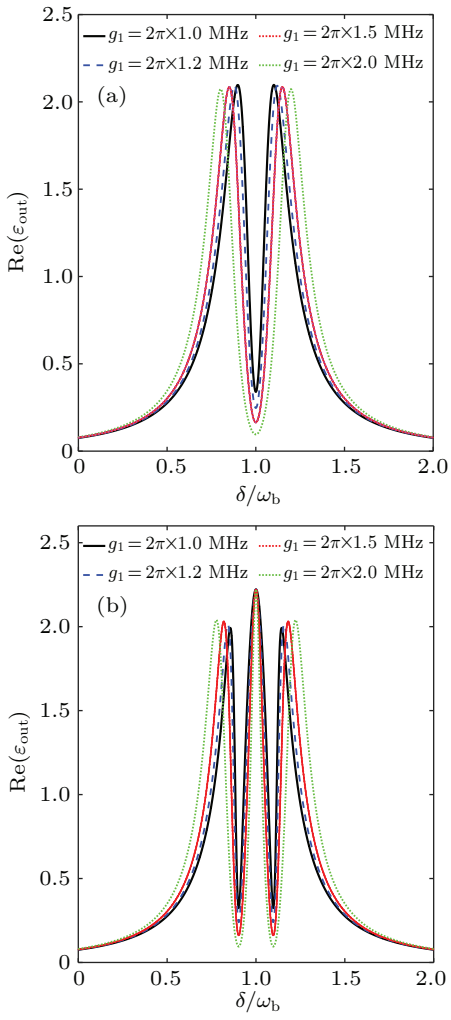


Fig. 2. Real part of the output field $\mathrm{Re}\,(\varepsilon_{\mathrm{out}})$ as a function of δ/ω_b for different values of the photon–magnon coupling strength g_1. (a) $G_a = 2\pi \times 1.0$ MHz, $G = 0$, (b) $G_a = 2\pi \times 1.0$ MHz, $G = 2\pi \times 1.0$ MHz.

In order to bring out prominently the effect of the atomic ensemble, we plot the absorption $\mathrm{Re}\,(\varepsilon_{\mathrm{out}})$ of the output field as a function of δ/ω_b for different values of the atom–cavity coupling strength G_a, when the value of the atomic ensemble decay rate is fixed. On the one hand, one can obtain that the sideband absorption peaks increase as the coupling of the atomic ensemble to the cavity increases, as shown in Fig. 3(a). The reason is that the radiation pressure is enhanced by increasing the atom–cavity coupling strength. The process is reversed in the case that the atom–cavity coupling strength G_a is fixed and the atomic dissipation γ_c is changed, as shown in Fig. 3(b).

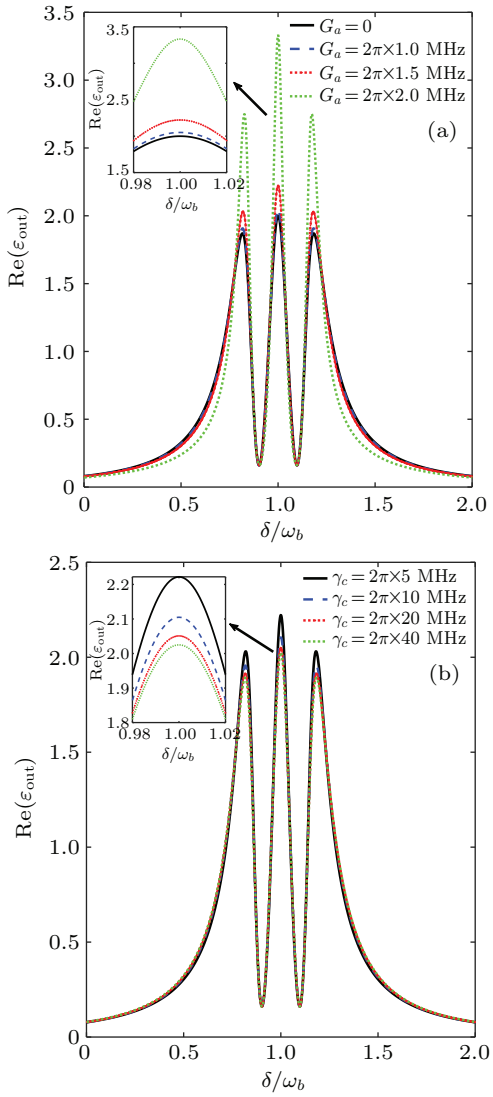


Fig. 3. Real part of the output field $\mathrm{Re}\,(\varepsilon_{\mathrm{out}})$ as a function of δ/ω_b. (a) The decay rate of atomic ensemble is fixed at $2\pi \times 5$ MHz, while the atom–cavity coupling strength G_a is varying. (b) The atom–cavity coupling strength is fixed at $G_a = 2\pi \times 1.0$ MHz, while the decay rate of the atomic ensemble is varying.

On the other hand, although different parameter G_a and γ_c are chosen, the widths of the two transparent windows are the same because the widths of the two transparent windows are only determined by the photon–magnon and magnon–phonon couplings and they are independent of other parameters. This indicates that the sideband peaks can be controlled by adjusting the parameters of the atomic ensemble. Furthermore, we plot the logarithm of the peak heights of the two absorption sides of the output spectrum as a function of the atom–cavity

coupling strength, as shown in Fig. 4. The value of the atom–cavity coupling strength can be easily detected by measuring the peak heights of the two absorption sides. It provides an effective and accurate method for measuring the atom–cavity coupling strength.

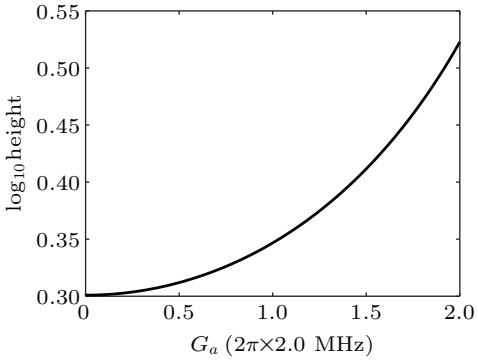


Fig. 4. The logarithm of the peak heights of the two absorption sides of the output spectrum versus the atom–cavity coupling strength.

3.2. Fano resonances in the output field

Then, we discuss the Fano resonances in the output spectrum. The output spectral shape of the Fano resonance is significantly different from the symmetric resonance curves in the EIT, MIT, OMIT and MMIT windows. In the system with optomechanical-like interactions, the reason for Fano resonance is the presence of non-resonant interactions. In our work, since the magnon mode is coupled to the phonon mode through an optomechanical-like interaction, this non-resonant interaction corresponds to $\tilde{\Delta}_m \neq \omega_b$. The absorption $\mathrm{Re}(\varepsilon_{\mathrm{out}})$ spectrum of probe field as a function of δ/ω_b is shown in Fig. 5.

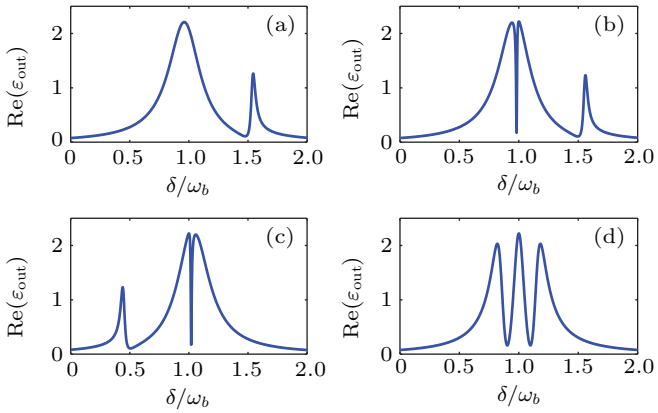


Fig. 5. Fano lineshapes in the asymmetric real part of the output field $\mathrm{Re}(\varepsilon_{\mathrm{out}})$ as a function of δ/ω_b, for $g_1 = 2\pi \times 1.5$ MHz, $G_a = 2\pi \times 1.0$ MHz: (a) $G = 0$, $\tilde{\Delta}_m = 1.5\omega_b$, (b) $G = 2\pi \times 1.0$ MHz, $\tilde{\Delta}_m = 1.5\omega_b$, (c) $G = 2\pi \times 1.0$ MHz, $\tilde{\Delta}_m = 0.5\omega_b$, (d) $G = 2\pi \times 1.0$ MHz, $\tilde{\Delta}_m = 1.0\omega_b$.

We can see from Figs. 5(a)–5(c) that the asymmetric Fano resonance occurs due to different non-resonant situations. In Fig. 5(a), we set the magnon–phonon coupling $G = 0$. The output spectrum appears with an asymmetric window profile, due to the existence of non-resonant process $\left(\tilde{\Delta}_m = 1.5\omega_b\right)$. Then, we introduce the magnon–phonon coupling. In Fig. 5(b), we can notice that the output spectrum is split into two absorption peaks with a narrow transparent window near $\delta = \omega_b$, which can be called MMIT. This illustrates that the magnon–phonon coupling produces the MMIT window. Further, we set the effective detuning value $\tilde{\Delta}_m$ of the driving field and magnon mode to $0.5\omega_b$. We can see from Fig. 5(c) that the Fano resonances peak moves from right $\left(\tilde{\Delta}_m = 1.5\omega_b\right)$ to left $\left(\tilde{\Delta}_m = 0.5\omega_b\right)$. In Fig. 5(d), Fano resonance disappears when we consider a resonance case $\tilde{\Delta} = 1.0\omega_b$.

3.3. The fast-slow light effects in the hybrid cavity magnomechanical system

We have discussed the magnomechanically induced transparency and Fano resonances of a hybrid cavity magnomechanical system. In the following, we investigate group delay of the output signal as a function of normalized probe field frequency δ/ω_b with different atom–cavity coupling strengths G_a. The group delay of the probe light is given by

$$\tau = \frac{\partial \phi}{\partial \omega_{\mathrm{p}}} = \mathrm{Im}\left[\frac{1}{\varepsilon_{\mathrm{out}}}\frac{\partial \varepsilon_{\mathrm{out}}}{\partial \omega_{\mathrm{p}}}\right] = \mathrm{Im}\left[\frac{1}{\varepsilon_{\mathrm{out}}}\frac{\partial \varepsilon_{\mathrm{out}}}{\partial \delta}\right]. \quad (18)$$

Physically, the positive (negative) value of group delay represents the occurrence of slow (fast) light transmission. According to Fig. 6, we can see that the maximum group delay increases significantly with the increase of the atom–cavity coupling strength G_a. The maximum and minimum group delays we can achieve are both about 17 μs. In the meantime, it is accompanied by a transition between fast and slow light near $\delta = 0.9\omega_b$ and $\delta = 1.1\omega_b$. The physical mechanism of group delay is the tunability quantum interference between the probe field and the anti-Stokes field. This suggests that the group delay can be dynamically adjusted to achieve modulation of fast and slow light by controlling the atom–cavity coupling strength.

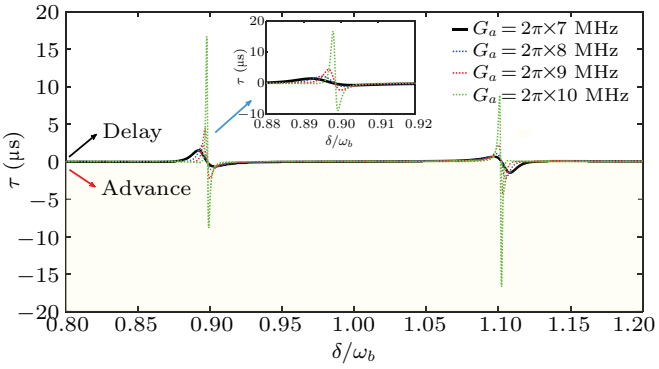


Fig. 6. The group delay τ of probe light as a function of δ/ω_b for different values of the atom–cavity coupling strength G_a.

Finally, we briefly analyze the experimental feasibility of the proposed model. The system of cavity trapping atomic ensemble has been carried out in the experiment.[62] The experiment that involves a highly polished single-crystal YIG

sphere interacting with a three-dimensional microwave cavity has been realized in Ref. [29]. A trapping of atoms experimentally[63] shows that the ground and excited atoms are not affected by the external magnetic field when they are in the proper position. Moreover, the frequency of the magnon is determined by the external bias magnetic field and therefore can be conveniently adjusted in a wide range.[29] Therefore, the current scheme based on a high-quality YIG sphere and an atomic ensemble placed inside a microwave cavity may be realizable in experiment.

4. Conclusion

In summary, we have investigated the absorption spectrum in a hybrid magnomechanical system. Due to the photon-magnon and phonon-magnon interactions, MMIT and MIT can be obtained in the absorption spectrum. The photon-magnon coupling can enhance MIT and MMIT. Then, we have explored the influence of atomic ensemble on the absorption spectrum. The results show that the better transparency effect can be achieved by choosing appropriate atomic ensemble parameters. In addition, we have proposed a method to measure the atom–cavity coupling strength. Furthermore, the phenomenon of Fano resonance due to the presence of anti-Stokes processes in the system is discussed in detail. Our study shows that the conversion between slow light and fast light can be achieved by modulating the atom–cavity coupling strengths appropriately. This study has some important guiding significance in the fields of high precision measurements and fabrication of optical devices.

Acknowledgements

Project supported by the National Natural Science Foundation of China (Grant No. 62061028), the Opening Project of Shanghai Key Laboratory of Special Artificial Microstructure Materials and Technology (Grant No. ammt2021A-4), the Foundation for Distinguished Young Scientists of Jiangxi Province (Grant No. 20162BCB23009), the Open Research Fund Program of the State Key Laboratory of Low-Dimensional Quantum Physics (Grant No. KF202010), the Interdisciplinary Innovation Fund of Nanchang University (Grant No. 9166-27060003-YB12), the Open Research Fund Program of Key Laboratory of Opto-Electronic Information Acquisition and Manipulation of Ministry of Education (Grant No. OEIAM202004), and the Graduate Innovation Special Fund of Jiangxi Province (Grant No. YC2021-S054).

References

[1] Weis S, Rivière R, Deléglise S, Gavartin E, Arcizet O, Schliesser A and Kippenberg T J 2010 *Science* **330** 1520
[2] Safavinaeini A H, Alegre T P, Chan J, Eichenfifield M, Winger M, Lin Q, Hill J T, Chang D E and Painter O 2011 *Nature* **472** 69
[3] Agarwal G S and Huang S 2010 *Phys. Rev. A* **81** 041803
[4] Liao Q H, Xiao X, Nie W J and Zhou N R 2020 *Opt. Express* **28** 5288
[5] Lei F C, Gao M, Du C G, Jing Q L and Long G L 2015 *Opt. Express* **23** 11508
[6] Zhang X Y, Zhou Y H, Guo Y Q and Yi X X 2018 *Phys. Rev. A* **98** 033832
[7] Boller K J, Imamoğlu A and Harris S E 1991 *Phys. Rev. Lett.* **66** 2593
[8] Fleischhauer M, Imamoglu A and Marangos J P 2005 *Rev. Mod. Phys.* **77** 633
[9] Paspalakis E and Knight P L 2002 *Phys. Rev. A* **66** 015802
[10] Wu Y and Yang X 2005 *Phys. Rev. A* **71** 053806
[11] Roghani M, Breuer H P and Helm H 2010 *Phys. Rev. A* **81** 033418
[12] Abdumalikov Jr A A, Astafiev O, Zagoskin A M, Pashkin Y A, Nakamura Y and Tsai J S 2010 *Phys. Rev. Lett.* **104** 193601
[13] Liao J Q, Wu Q Q and Nori F 2014 *Phys. Rev. A* **89** 014302
[14] Mancini S, Giovannetti V, Vitali D and Tombesi P 2002 *Phys. Rev. Lett.* **88** 120401
[15] Gao M, Lei F C, Du C G and Long G L 2016 *Sci. China Phys. Mech.* **59** 610301
[16] Marangos J P 1998 *J. Mod. Opt.* **45** 471
[17] Jiang C, Liu H X, Cui Y S, Li, X W and Chen G B 2013 *Opt. Express* **21** 12165
[18] Wu S C, Qin L G, Jing J, Yan, T M and Lu J 2018 *Phys. Rev. A* **98** 013807
[19] Han Y, Cheng J and Zhou L. 2011 *J. Phys. B: At. Mol. Opt. Phys.* **44** 165505
[20] Li X Y, Nie W J, Chen A X and Lan Y H 2018 *Phys. Rev. A* **98** 053848
[21] Huebl H, Zollitsch C W, Lotze J, Hocke F, Greifenstein M, Marx A, Gross R and Goennenwein S T B 2013 *Phys. Rev. Lett.* **111** 127003
[22] Tabuchi Y, Ishino S, Ishikawa T, Yamazaki R, Usami K and Nakamura Y 2014 *Phys. Rev. Lett.* **113** 083603
[23] Zhang X F, Zou C L, Jiang L and Tang H X 2014 *Phys. Rev. Lett.* **113** 156401
[24] Goryachev M, Farr W G, Creedon D L, Fan Y H, Kostylev M and Tobar M E 2014 *Phys. Rev. Appl.* **2** 054002
[25] Bai L, Harder M, Chen Y P, Fan X, Xiao J Q and Hu C M 2015 *Phys. Rev. Lett.* **114** 227201
[26] Zhang D, Wang X M, Li T F, Luo X Q, Wu W D, Nori F and You J Q 2015 *npj Quantum Inf.* **1** 15014
[27] Zhang X F, Zhu N, Zou C L and Tang H X 2016 *Phys. Rev. Lett.* **117** 123605
[28] Soykal Ö O and Flatté M E 2010 *Phys. Rev. Lett.* **104** 077202
[29] Zhang X F, Zou C L, Jiang L and Tang H X 2016 *Sci. Adv.* **2** e1501286
[30] Potts C A, Varga E, Bittencourt V A S V, Kusminskiy V S and Davis J P 2021 *Phys. Rev. X* **11** 031053
[31] Tabuchi Y, Ishino S, Noguchi A, Ishikawa T, Yamazaki R, Usami K and Nakamura, Y 2015 *Science* **349** 405
[32] Nair J M P and Agarwal G S 2020 *Appl. Phys. Lett.* **117** 084001
[33] Li J, Zhu S Y and Agarwal G S 2018 *Phys. Rev. Lett.* **121** 203601
[34] Li J and Zhu S Y. 2019 *New J. Phys.* **21** 085001
[35] Ullah K, Naseem M T and Müstecaplıoğlu Ö E 2020 *Phys. Rev. A* **102** 033721
[36] Yang Z X, Wang L, Liu Y M, Wang D Y, Bai C H, Zhang S and Wang H F 2020 *Front. Phys.* **15** 52504
[37] Kani A B, Sarma and Twamley J 2022 *Phys. Rev. Lett.* **128** 013602
[38] Lu T X, Zhang H L, Zhang Q and Jing H 2021 *Phys. Rev. A* **103** 063708
[39] Lü H, Wang C Q, Yang L and Jing H 2018 *Phys. Rev. Appl.* **10** 014006
[40] Li X, Yang W X, Shui T, Li L, Wang X and Wu Z 2020 *J. Appl. Phys.* **128** 233101
[41] Kong C, Wang B, Liu Z X, Xiong H and Wu Y 2019 *Opt. Express* **27** 5544
[42] Wang Y P, Zhang G Q, Zhang D K, Li T F, Hu C M and You J Q 2018 *Phys. Rev. Lett.* **120** 057202
[43] Wang Y P, Rao J W, Yang Y, Xu P C, Gui Y S, Yao B M, You J Q and Hu C M 2019 *Phys. Rev. Lett.* **123** 127202
[44] Shen R C, Li J, Fan Z Y, Wang Y P and You J Q 2022 *Phys. Rev. Lett.* **129** 123601
[45] Qiu W Y, Cheng X H, Chen A X, Lan Y H and Nie W J 2022 *Phys. Rev. A* **105** 063718
[46] Li S Y and Zhu A D 2022 *Ann. Phys.* **534** 2100609
[47] Zhao C S, Li X, Chao S L, Peng R and Li C 2020 *Phys. Rev. A* **101** 063838

[48] Huai S N, Liu Y L, Zhang J, Yang L, Liu and Y X 2019 *Phys. Rev. A* **99** 043803
[49] Wang L, Yang Z X, Liu Y M, Bai C H, Wang D Y, Zhang, S and Wang H F 2020 *Ann. Phys.* **532** 2000028
[50] Bi M X, Yan X H, Zhang Y and Xiao Y 2021 *Phys. Rev. B* **103** 104411
[51] Zhao C O, Peng R, Yang Z, Chao S L, Li C, Wang Z H and Zhou L 2022 *Phys. Rev. A* **105** 023709
[52] Ding M S, Zheng L and Li C 2019 *Sci. Rep.* **9** 15723
[53] Lachance-Quirion D, Tabuchi Y, Gloppe A, Usami K and Nakamura Y 2019 *Appl. Phys. Express* **12** 070101
[54] Wang K, Gao Y P, Jiao R and Wang C A 2022 *Front. Phys.* **17** 42201
[55] Yuan H Y, Cao Y S, Kamra A, Duine R A and Peng Y 2022 *Phys. Rep.* **965** 1
[56] Xiao X, Liao Q H, Zhou N R, Nie W J and Liu Y C 2020 *Sci. China Phys. Mech.* **63** 114211
[57] Chen B, Shang L, Wang X F, Chen J B, Xue H B, Liu X and Zhang J 2019 *Phys. Rev. A* **99** 063810
[58] Liu Z X, Xiong H, Wu M Y and Li Y Q 2021 *Phys. Rev. A* **103** 063702
[59] Kippenberg T J and Vahala K J 2007 *Opt. Express* **15** 17172
[60] Huang S and Agarwal G S 2011 *Phys. Rev. A* **83** 043826
[61] Yellapragada K C, Pramanik N, Singh S and Lakshmi P A 2018 *Phys. Rev. A* **98** 053822
[62] Hernandez G, Zhang J P and Zhu Y F 2007 *Phys. Rev. A* **76** 053814
[63] Raab E L, Prentiss M, Cable A, Chu S and Pritchard D E 1987 *Phys. Rev. Lett.* **59** 2631